Acta Astronautica 81 (2012) 419–429

Contents lists available at SciVerse ScienceDirect

Acta Astronautica

journal homepage: www.elsevier.com/locate/actaastro

Plastic Cubesat: An innovative and low-cost way to perform applied space research and hands-on education ☆

Jacopo Piattoni [a,*], Gian Paolo Candini [a], Giulio Pezzi [a], Fabio Santoni [b], Fabrizio Piergentili [c]

[a] University of Bologna "ALMA MATER", II Faculty of Engineering, Forlì (FC), Italy
[b] Dipartimento di Ingegneria Astronautica, Elettrica ed Energetica-DIAEE, Universita' di Roma "La Sapienza", Roma, Italy
[c] Department of Mechanical and Aerospace Engineering, University of Rome "La Sapienza", Roma, Italy

ARTICLE INFO

Article history:
Received 28 February 2012
Received in revised form
22 July 2012
Accepted 25 July 2012
Available online 12 October 2012

Keywords:
Cubesat
Plastic
Rapid prototyping
Micro attitude control
Embedded antenna.

ABSTRACT

This paper describes the design and the manufacturing of a Cubesat platform based on a plastic structure.

The Cubesat structure has been realized in plastic material (ABS) using a "rapid prototyping" technique. The "rapid prototyping" technique has several advantages including fast implementation, accuracy in manufacturing small parts and low cost. Moreover, concerning the construction of a small satellite, this technique is very useful thanks to the accuracy achievable in details, which are sometimes difficult and expensive to realize with the use of tools machine. The structure must be able to withstand the launch loads. For this reason, several simulations using an FEM simulation and an intensive vibration test campaign have been performed in the system development and test phase. To demonstrate that this structure is suitable for hosting a complete satellite system, offering innovative integrated solutions, other subsystems have been developed and assembled.

Despite its small size, this single unit (1U) Cubesat has a system for active attitude control, a redundant telecommunication system, a payload camera and a photovoltaic system based on high efficiency solar cells.

The developed communication subsystem has small dimensions, low power consumption and low cost. An example of the innovations introduced is the antenna system, which has been manufactured inside the ABS structure. The communication protocol which has been implemented, the AX.25 protocol, is mainly used by radio amateurs. The communication system has the capability to transmit both telemetry and data from the payload, in this case a microcamera.

The attitude control subsystem is based on an active magnetic system with magnetorquers for detumbling and momentum dumping and three reaction wheels for fine control. It has a total dimension of about $50 \times 50 \times 50$ mm. A microcontroller implements the detumbling control law autonomously taking data from integrated magnetometers and executes pointing maneuvers on the basis of commands received in real time from ground.

The subsystems developed for this Cubesat have also been designed to be scaled up for larger satellites such as 2U or 3U Cubesats. The additional volume can be used for more complex payloads. Thus the satellite can be used as a low cost platform for companies, institutions or universities to test components in space.

© 2012 Elsevier Ltd. All rights reserved.

☆ This paper was presented during the 62nd IAC in Cape Town.

* Corresponding author. Tel.: +49 15777802477.
E-mail addresses: jacopo.piattoni@gmail.com (J. Piattoni), gpaolo79@gmail.com (G.P. Candini), labwebmode@gmail.com (G. Pezzi), fabio.santoni@uniroma1.it (F. Santoni), Fabrizio.piergentili@uniroma1.it (F. Piergentili).

0094-5765/$ - see front matter © 2012 Elsevier Ltd. All rights reserved.
http://dx.doi.org/10.1016/j.actaastro.2012.07.030

1. Introduction

This paper describes the design and the manufacturing of a Cubesat platform realized within the activities of the Space Robotics Laboratory and V-Lab of the II Faculty of Engineering of Bologna University in collaboration with the AeroSpace System Laboratory of the University of Rome "La Sapienza".

It is a satellite of cubic shape (10 cm per side), weighing approximately 1 kg, based on the creation of a central body made entirely of plastic material using the Rapid Prototyping Techniques [1–7].

The aim of the work is to realize a multipurpose low-cost cubesat platform, easy to adapt to different possible nanopayloads, suitable for potential aerospace research applications, such as microcameras, electronic components to be tested and space weather monitoring sensors. The requirements for the Cubesat have been set considering a standard Low Earth Orbit environment with a half orbit eclipse period and a lifetime of 1 year. The typical launcher environmental conditions have been chosen considering a possible low cost solution for this kind of satellite, represented by the Indian PSLV launch vehicle.

Particular attention has been given to the structural analysis since the material used for rapid prototyping has never been tested in space, and an intensive ground test campaign has been carried out. The results of these tests are highlighted in the paper.

The power system is based on triple junction small solar cells. The telecommunication system uses components usually employed for terrestrial uses and adapted to the space environment.

In the final part of the paper an extensive overview of the miniaturized attitude control system, specifically designed for this kind of nanosatellite, will be given.

2. Satellite overview

The Cubesat under development will permit us to test the effectiveness of using structures manufactured with the rapid prototyping techniques in orbit and the performance of the new miniaturized attitude control system, evaluating its reliability and endurance.

The Cubesat will host a camera as the main payload, already used on board stratospheric balloons, in the framework of the AURORA experiment [9,10], flown from Kiruna thanks to the ESA REXUS/BEXUS project [11], which passed the thermovacuum test at ESA ESTEC facilities. This is a COTS camera usually employed in terrestrial industrial applications. Using different COTS optics it is possible to change the field of view and resolution of the system adapting it to the specific mission. The camera can take color pictures with a resolution of 640×480 pixels and can provide them directly in the JPEG compressed format, saving on-board computation efforts and memory. The characteristics that have determined the choice of this microcamera are its small dimensions, about $20 \times 28 \times 11$, and the weight, about 30 g.

3. Satellite structure

To respect the specifications of the 1U Cubesat, many restrictions are present, especially on the external dimensions [9].

The structure is designed as a cube with 100 mm side, with square columns (8.5 mm side and 113.5 mm height), placed at four parallel corners. The structure has a front access point and an opening in the top side, to allow the assembly and accessibility of internal parts (Fig. 1).

The structure is realized by exploiting a rapid prototyping technique. This choice allows us to optimize the design and the construction of a Cubesat.

Usually rapid prototyping techniques are used to build the prototype of a product; the aim of this paper is to investigate the suitability of using this technique for the final product manufacturing. The advantages of this manufacturing technique are the possibility to produce very complex shapes, which would be expensive or impossible to achieve using traditional production methods, short manufacturing time and low costs.

Moreover, this material has a density lower than aluminum (ABS$=1.05$ g/cm^3; aluminum$=2.7$ g/cm^3), this allows for potential mass savings. This technique changes the usual idea of primary and secondary structure because the whole part is produced at the same time, thus reducing the number of parts and the need for screwing and gluing, also increasing the reliability of the structure. This simplifies also the assembling phase. Traditional manufacturing techniques usually remove

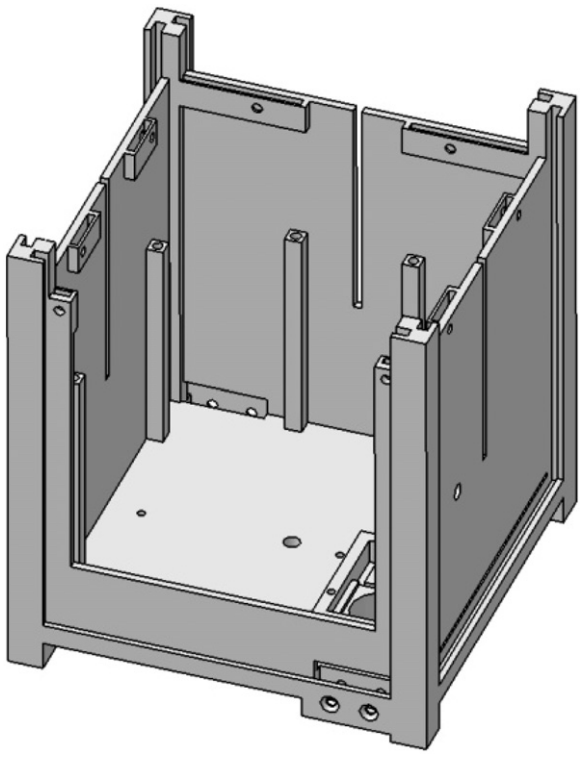

Fig. 1. Complete structure.

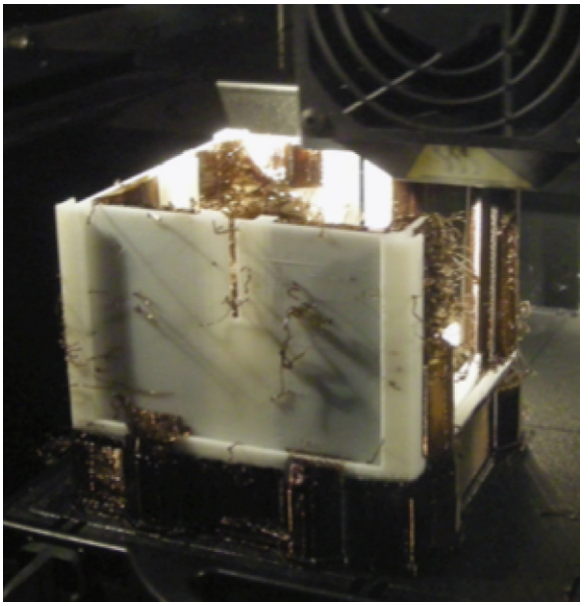

Fig. 2. Rapid prototyping machine during the building of the structure.

material from a metallic base. Rapid prototyping, on the contrary, adds material, layer by layer (Fig. 2).

The technique chosen is the FDM (Fused Deposition Modeling) that deposes a very thin wire of plastic material. One of the disadvantages is that in this way the material is not isotropic. On the other hand, it offers the possibility of optimizing the deposition direction, on the basis of maximum load preferential directions. After the production, the part can also be worked in order to obtain specific effect, as the reduction of the roughness.

Body-mounted solar panels and a top cover, also equipped with a solar panel, close the satellite sides. The top cover is also made of ABS.

A disadvantage is the impossibility of obtaining threaded holes. Two solutions to this problem were found: (1) the use of screws long enough to be bolted, in the points where it is possible to access both sides of the screw and (2) in situations where this is not possible, the creation of pockets in which small aluminum inserts are placed in order to provide the lock.

The most critical environmental tests were performed and the critical components selected according to the orbital environment requirements. Vacuum tests and thermal cycling were performed on the structure and no considerable changes in structure mass were recorded, showing material outgassing lower than 1% of the total structure mass after cure cycle simulating LEO orbit conditions (about one orbital period, temperature varying between -20° and 80°). Moreover, the structure was submitted to a thermal shock test and it was resistant to sudden temperature changes (cycles were performed between $-20\,^{\circ}$C and $60\,^{\circ}$C).

The effect of radiation on ABS is considered negligible, since from Ref. [14], it results that the total dose requested to have severe damages on structure is on the order of 10^9 rad(Si), extremely larger than any LEO satellite experiments in 1 year of orbital operations (lower than 10^7 at 2000 km height [15]). Concerning the direct solar light it must be considered that the structure is almost completely covered with solar cells which shield the main part of the ABS structure.

Two electronic boards (Communication and On Board Data Handling system) are mounted on an aluminum plate at the top of the satellite. In this way the two boards, which are the most sensitive components, are isolated from the rest of the on-board systems (Fig. 3) and the aluminum helps by dissipating the heat from the electronic boards which is in the order of 1 W during transmission.

A numerical analysis has been carried out to validate the structure. A numerical model with 15,000 elements has been realized, representing the satellite fixed to the interface through the four lateral columns, as usual for P-Pod for Cubesat launch [9]. The analysis has been performed using the software Nastran and Patran as pre and post processor. The material as been simulated as 3d orthotropic [8].

The numerical analysis aimed to evaluate the stresses of the structure by performing the Power Spectral Density (PSD) test characterized through the launcher parameters (Table 2). This test was used to evaluate Von Mises stresses which resulted on the order of 10^4 Pa, thus one order of magnitude lower than the ABS maximum acceptable which is on the order of 10^5 Pa. Stress distribution on the cover (the most stressed part) is shown in Fig. 4.

The vibration tests carried out on the shaker platform aimed at qualifying the structure for launch. During the tests the typical vibration profiles of the launch environment were simulated. The parameters of the PSLV rocket, of the ISRO (Indian Space Research Organization), have been considered as representative of the launch environment.

The tests performed include "sine sweep" and "random" vibration testing; as summarized in Table 1.

Two identical sine sweep sessions were carried out, before and after the random vibration testing, to evaluate possible structural performance degradation induced by the launch loads.

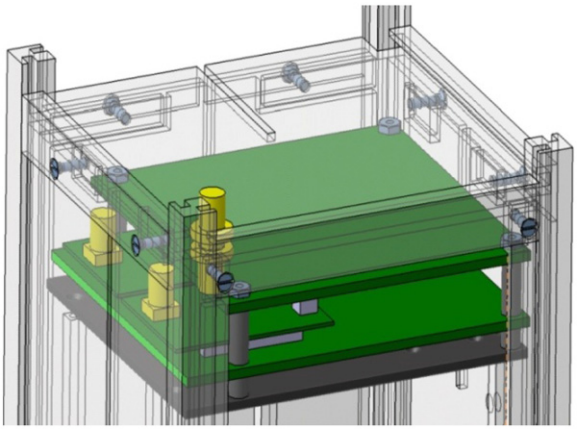

Fig. 3. On-board electronic boards.

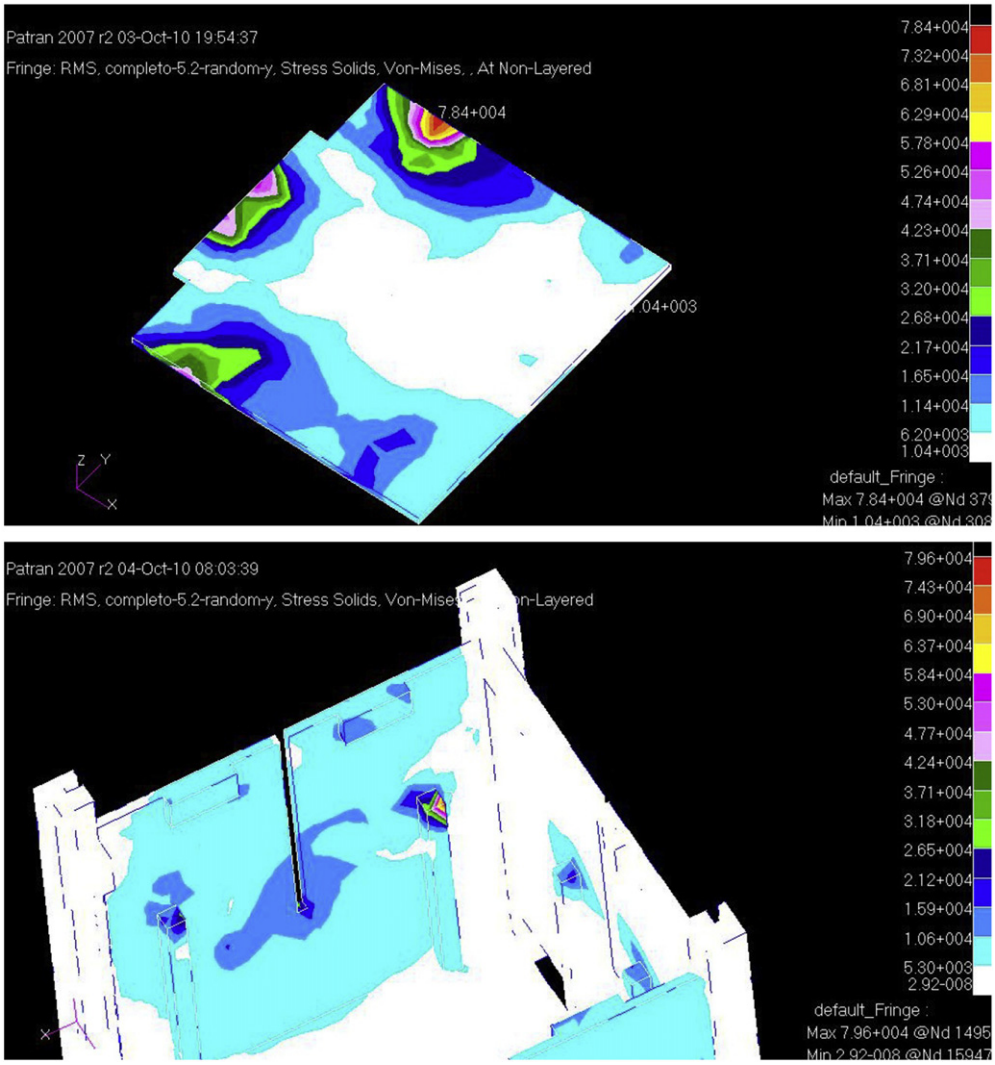

Fig. 4. Cubesat numerical analysis—PSD Von Mises stresses on cover (upper picture) and side (lower picture).

Table 1
Vibration test settings.

1° sine sweep	5–400 Hz, 1 g,…, 2 oct/min 5–10 Hz, 12.5 mm,…, 2 oct/min 10–100 Hz, 2.5 g,…, 2 oct/min
PSD	see Table 2
2° sine sweep	5–400 Hz, 1 g,…, 2 oct/min 5–10 Hz, 12.5 mm,…, 2 oct/min 10–100 Hz, 2.5 g,…, 2 oct/min

Three points were monitored by accelerometers during the tests: the lid of the structure (triaxial), one of the lateral panels (monoaxial), and base of the test-pod (monoaxial).

The picture in Fig. 5 shows the triaxial sensor mounted on the satellite lid.

Once the sensors were fixed the Cubesat was inserted into the test-pod. The sensors used were chosen on the basis of their lightness in order to avoid any considerable

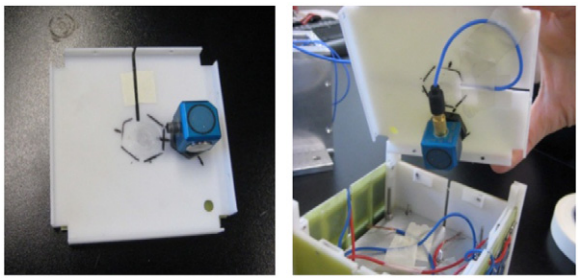

Fig. 5. Placement of lid sensor.

effect on the satellite structure inertia tensor and simulating real masses which will be attached to the structure. Various different tests were performed in different positions in order to identify the real critical modes of the structure. Fig. 6 shows the triaxial sensor axes orientation.

Fig. 7 shows the test-pod fixed to the head of the shaker; the image also shows the other two sensors used

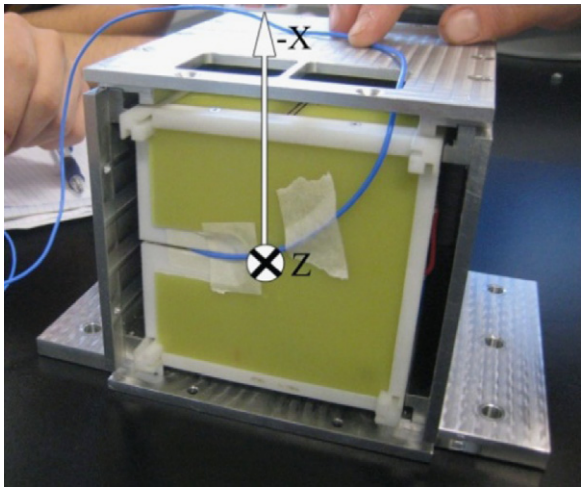

Fig. 6. Orientation of the axes in the lid sensor.

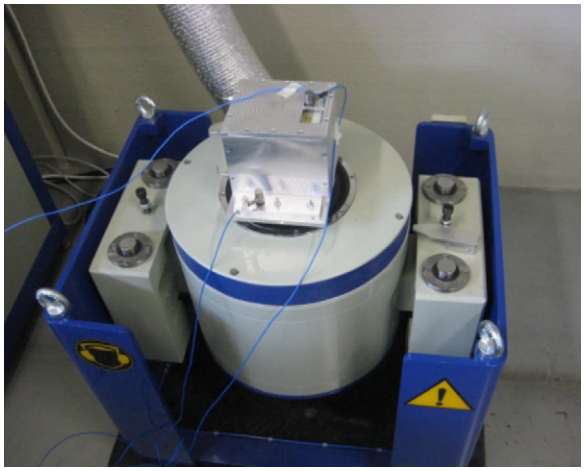

Fig. 7. Test-pod mounted on the top of the shaker.

for tests: the monoaxial accelerometer mounted on the fiberglass panel and the monoaxial feedback sensor set at the base of the test-pod.

The two monoaxial sensors measure accelerations in the vertical direction, which is the movement direction of the shaker head. Results of the vibration test along the most stressed direction (x) are discussed hereafter.

- Sine sweep 5–400 Hz, 1 g: this test allows us to evaluate the natural frequency of the structure. The presence of a peak indicates that the monitored component has reached the resonance frequency. The most critical responses were recorded by the triaxial accelerometer mounted beneath the cover lid in the $-x$ axis, the direction parallel to the displacement of the shaker head. The frequency is the same even after random vibrations (Fig. 8). The responses demonstrate that the structure complies with PSLV stiffness specifications.
- Sine sweep 5–10 Hz, 12.5 mm: this test was carried out in order to estimate the behavior of the structure during low frequency excitements. These frequencies produce the higher displacement; this is why it was possible to use this test to qualify the structure to quasi-static loads. The graphs obtained show that in the direction parallel to the movement of the head of the shaker, acceleration increases with the frequency. In the cover lid the amplitude reaches a maximum value of 5.30 g. The trend of the curves is the same before and after the PSD stress (Fig. 9).
- Sine sweep 10–100Hz, 2.5g: this test is the last of the sinusoidal vibration qualification program. Even in this case the amplitude of the measured response increases with the increase of frequency. The cover lid of the structure is the most stressed component. Starting from a value of 2.5 g the curve reaches an amplitude of 4 g, when the frequency is 100 Hz. The red curve of the post PSD test has the same trend (Fig. 10).

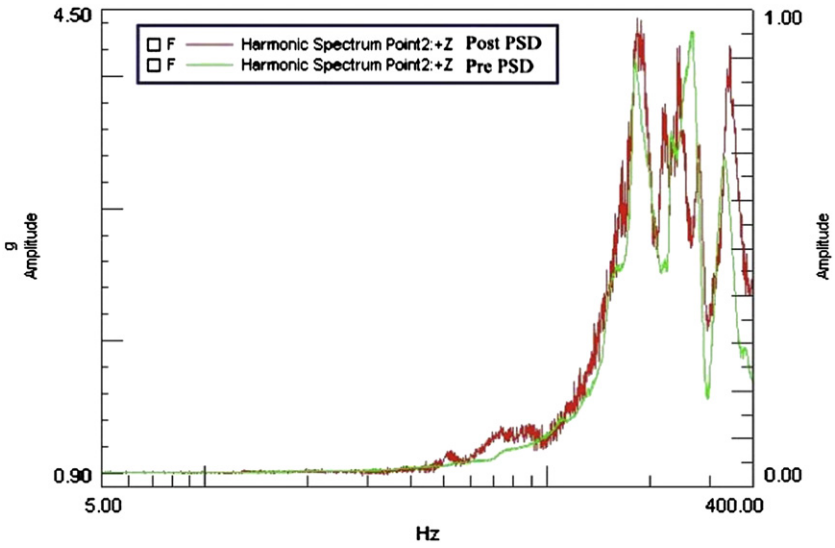

Fig. 8. Pre/post PSD comparison between the responses of the lid during 5–400 Hz test ($-x$ axis).

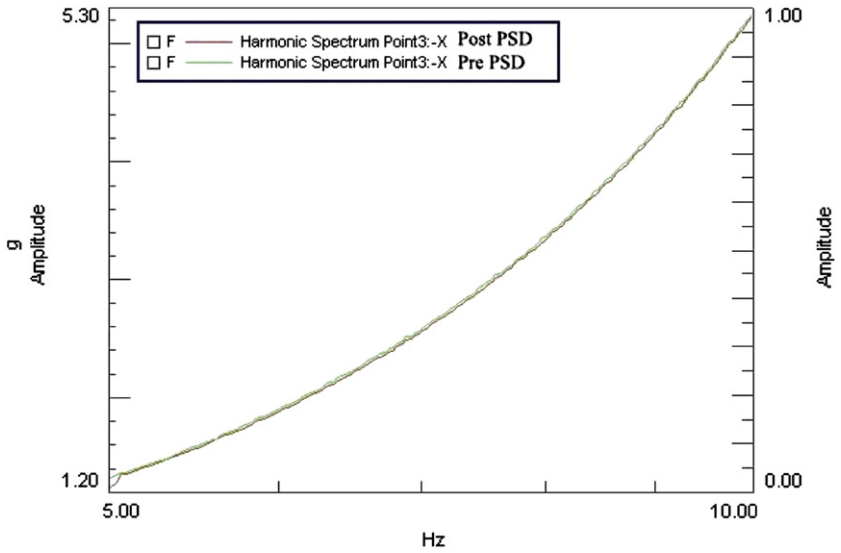

Fig. 9. Pre/post PSD comparison between the responses of the lid during 5–10 Hz test ($-x$ axis).

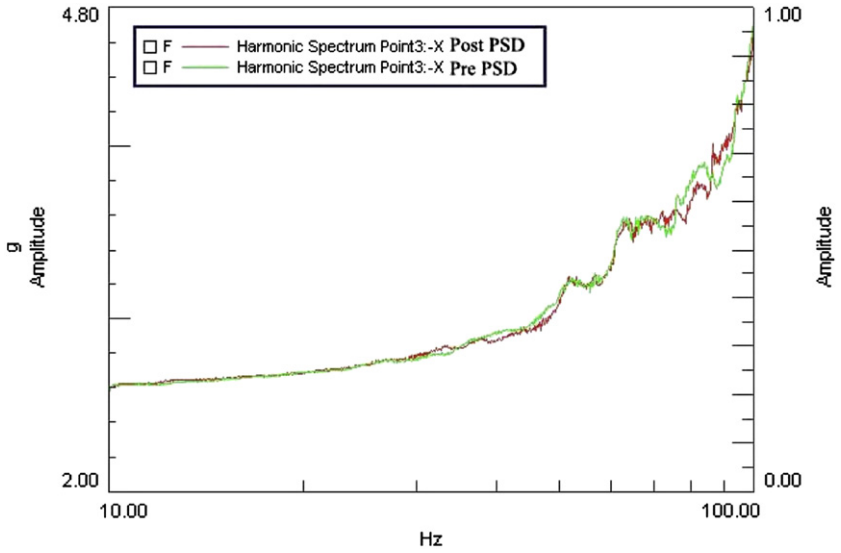

Fig. 10. Pre/post PSD comparison between the responses of the lid during 10–100 Hz test ($-x$ axis).

After the tests a visual inspection of the structure was carried out. No damage or alterations were detected in the external structure or in the inner components. The analysis of the results showed that the structure is capable of sustaining the stress experienced during the launch, without damage and complying with the requirements imposed by the PSLV rocket, especially the stiffness criteria. The pre/post PSD responses measured by the accelerometers showed very similar results.

4. Power system

To provide the power needed on board, there are two sources: secondary batteries and solar panels.

The power sub-system architecture is very simple. The solar arrays are directly connected to the battery, through a blocking diode. In this configuration the solar panel voltage must be higher than the battery voltage.

Thus, the requirement for the power system design is: bus voltage higher than 6 V (transmitter requirement) and as much power as possible.

To this purpose, a battery pack consisting of six NiCd batteries connected in series was assembled. Each battery cell has a nominal voltage of 1.2 V for a total bus voltage of 7.2 V. The batteries are recharged by solar panels mounted on the body of the satellite. The chosen solar cells are TASC, (Triangular Advanced Solar Cell), produced by Spectrolab. These are triple junction solar cells, providing 1.8 V voltage in the operating illumination and temperature range. The solar cells are mounted in series in strings of four, to provide 7.2 V. They are connected in series using an adhesive tin aluminum strip and they are

glued to fiberglass panels. These panels are mounted on the satellite structure by inserting them in rails specifically designed and built in the ABS structure, internal to the satellite columns.

An accurate glue deposition is required for solar cell bonding to the fiberglass panel. This is obtained by using an adhesive mask that reproduces the solar array layout (Fig. 11).

The glue used is a commercial off-the-shelf, extended temperature range silicone, rated for operation between −40 °C and 80 °C. The same technique has already been used on other microsatellites [12,13].

Each panel is divided into four quadrants, each one containing an array of four series connected solar cells. The complete solar panel, including four solar cell strings, is shown in Fig. 12.

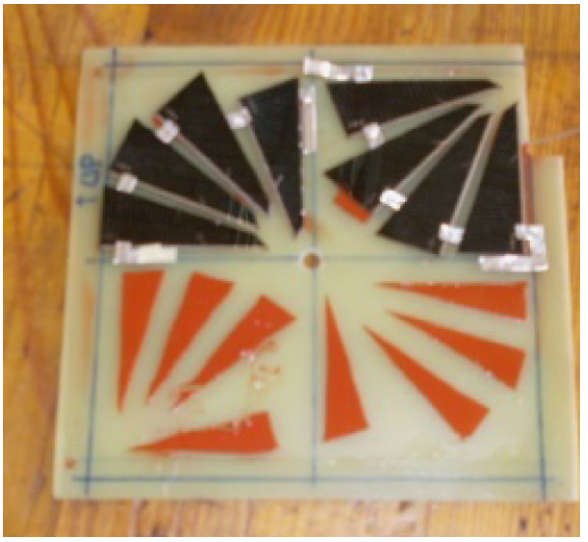

Fig. 11. Gluing mask.

Fig. 12. Solar panels glued onto the fiberglass panel.

The lower face of the satellite does not host any solar panels, due to the presence of the camera and bolts necessary for the Cubesat assembly.

5. Communication system

The communication system is based on two commercial off the shelf transceivers, one used as a receiver and the other as a transmitter. The presence of two transceivers ensures a certain level of redundancy and permits operation in full duplex in downlink and uplink. They are both CC1020 models. The first one is always kept on for receiving commands from the ground. The second one, used for transmission, is activated only when the satellite receives the appropriate command signal from the ground station. This procedure ensures that transmission will be performed only in the visibility of the ground stations, saving on-board power.

The CC1020 is an FSK-GFSK Narrowband low power UHF wireless data transmitter and receiver with channel spacing as low as 12.5 and 25 kHz. The GFSK modulation has been selected to enhance the bandwidth utilization efficiency.

The data rate is 1.2 Kbaud GFSK with an RF power of 2 W. The decision has been taken to use 2 UHF frequencies for downlink because of the configuration of one of the transceivers as a receiver with a low noise amplifier in the front end and the other one as a transmitter with a dedicated Power Amplifier.

Having two on-board transceivers requires either the presence of two separate antennas, or the use of a diplexer or commutation system to prevent transmission power reaching the receiver if a configuration with a single antenna is used. The first solution has been chosen.

The transmission antenna is made of a conductive material with good shape memory, about 20 cm long. It will be wrapped around the satellite and locked in the closed position by a wire connected through a hole in the structure to a thermal cutter. Obviously the simpler the path of the wire, the more the reliability of the system increases: for this reason the cutter has been installed on a suitable aluminum support in proximity of the hole through which the wire passes. The thermal cutter system has already been tested on board the REXUS 7 rocket with the BUGS experiment [10,11].

The antenna is connected to the transmitter via a connector located on the satellite lid, as shown in Fig. 13. For the receiving antenna, the rapid prototyping technique offers the possibility to embed it inside the satellite structure itself, since it is not conductive.

A prototype platform with receiving and transmitting systems has already been developed and tested. Both systems are shown in Fig. 14.

6. Attitude control system

The mission will also be used to test a newly developed miniaturized attitude controller, suitable for microsatellites and Cubesats. The attitude controller comprises three reaction wheels, three magnetic actuators for angular velocity stabilization and reaction wheel desaturation and a three axis magnetometer. The system is built to be

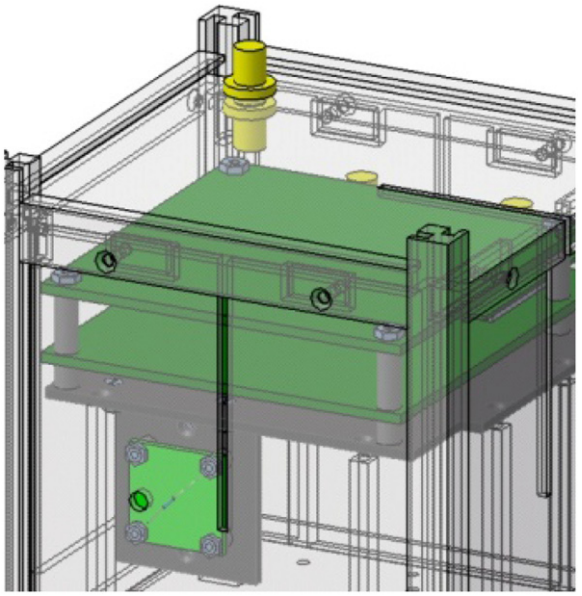

Fig. 13. Thermal cutter and connector of transmitting antenna.

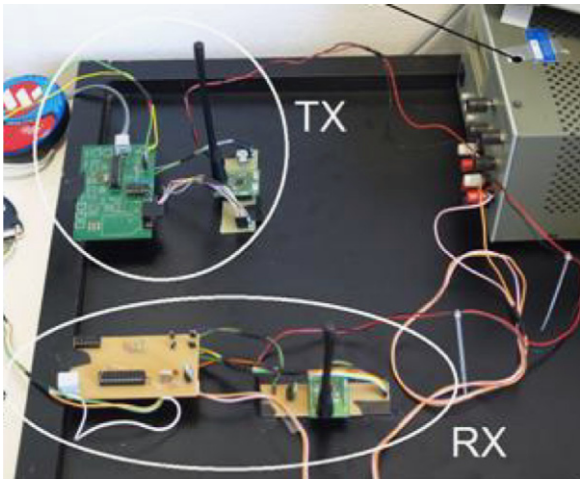

Fig. 14. Test of transmission and receiving prototypal systems.

compatible with the size of a 1U Cubesat, but sized to be installed even on larger microsatellites. The complete size of the system is a 52 mm cube.

With a 1U cubesat of $100 \times 100 \times 100$ mm, the use of 1/8 of the volume was considered a good tradeoff between the space needs for the attitude control system and the space for the payloads. The mass requirement is less restrictive than the volume one.

The momentum wheels design has also been driven mainly by dimension constrains to be used on cubesat satellite. This system will be briefly described, focusing mainly on the characteristics of the developed prototype.

6.1. Requirements and solutions

Cubesats and more generally small low-cost satellites include all basic subsystems for their missions, but usually lack more sophisticated systems, like active attitude control, due to both space and cost limitations.

A system capable of combining the low-cost characteristics of the typical microsatellite application and the small size required by this class of spacecraft would open up new possibilities for experiments that require the control of satellite attitude along the orbit.

The developed system includes: (i) magnetic control, to be used in the first stage of the orbit and capable of damping the initial tumbling motion due to the release of the satellite and for reaction wheel desaturation; (ii) reaction wheels, used for attitude maneuvers; and (iii) attitude sensors, to be used for attitude determination. The system has been designed as a self-contained unit, to be installed onboard nanosatellites, such as Cubesats, as a building block for the satellite system and working independently from the host spacecraft, except for power and command or data exchange. The main requirement is the physical size of the miniaturized ACS. The prefixed target is a cube with a side of about 5 cm. Despite the small space available, it is necessary to include all of the required ACS subsystems inside this volume. No particular requirements have been fixed on the system mass and power, as long as the final design is compliant with the typical Cubesat on-board resources. Since standard values are not established for this class of satellites, the driving criterion has been to keep mass and power as low as possible.

The requirements concerning the attitude control performance have been defined in terms of total angular momentum storage and maneuvering capability. The first requirement is that the maximum angular momentum storage corresponds to the environmental torque effects in one orbit, assuming the worst case condition of maximum continuous torque and absence of desaturation maneuvers in this time span. The attitude maneuvers requirement has been fixed such that a single Cubesat, with moment of inertia of about 0.01 Kg m^2, performs a 180° rest-to-rest turn in less than 1 min.

On the control electronics, requirements have been imposed to create a system capable of executing real time commands, such as orbital maneuvers and autonomous control, such as attitude stabilization after being released from the launcher.

As a technological implementation requirement, the system should be composed of commercial off-the-shelf terrestrial components.

The magnetorquers have been designed based on the main constraint of being 40 mm in length, to fit inside the volume assigned to the ACS. Hence a suitable high permeability rod has been selected among those commercially available with the required maximum length and nominal magnetic permeability of 2300. A bar of 6 mm in diameter, taking into account for demagnetization, has an apparent permeability of about 3.27×10^{-5} Wb/(Am). Since the required magnetic dipole is 0.018 Am^2, and the bar volume is 1131 mm^3, the required magnetizing field for the magnetorquer is 7.8 Oe, which can be obtained by a 500 turns solenoid wound on the rod and 50 mA current.

Three perpendicular magnetorquers, 4 cm long and 6 mm wide with 50 mA of current would provide a good

tradeoff between size and torque available, as demonstrated by numerical simulation.

Reaction wheels have been designed according to the strong constrains on size derived from the volume assigned to the control system. To power the wheels a brushless micro-motor produced by Faulhaber has been selected. It is characterized by an extremely reduced size, with only 2 mm of thickness and 1 cm of diameter, high nominal rotation speed and low power.

According to datasheet characteristics, the motor can provide a maximum torque of 0.16 mNm and a no-load speed of 41,000 rpm. A nominal power supply voltage of 4 V makes it compatible with the control signal at 3.3 V.

The Integrated ACS has been dimensioned for attitude pointing and fast maneuvers.

The microwheels have been designed considering the possibility to use the system not only on 1U Cubesats, but also on 3U Cubesats. The typical maximum value of the environmental torque magnitude for a 3U Cubesat in a circular polar orbit at 500 km can be evaluated as 13.6e-8 Nm. So the requirements on maximum total angular momentum accumulated in one orbit due to the environmental torque magnitude for a triple Cubesat in a circular polar orbit at 500 km, about 5700 s, has been considered roughly 8×10^{-4} Nm s.

The motor torque has been chosen on the basis of the maneuvering requirements. It is assumed that the system, installed on a 3U Cubesat, is capable of performing a 180° rest-to-rest maneuver in 1 min.

The system integrates a three axis magnetometer, used to collect the necessary data for the control law and also suitable for earth magnetic field measurement.

The core of the control system is based on a Microchip DSPic device, providing high speed serial communication, fast data processing and enough memory for a full functioning program.

All the functioning parameters of the internal functions, such as gains and filter frequencies, can be changed by the user according to the environment where the system is working. For the performed simulations, the -Bdot sampling rate was fixed at 2 Hz, using an average filtering on multiple sampling at each calculation point.

6.2. Prototype

The building of the prototype has been preceded by a series of numerical simulations to verify the capabilities of the designed system. These simulations have been performed with the following scenario:

- circular orbit at 700 km of height;
- satellite moment of inertia as [0.01, 0.01, 0.01] Kg m^2;
- maximum current of magnetorquers: 50 mA;
- maximum momentum wheel speed 6600 rpm.

All simulations have indicated the capability of the control system to perform all requested maneuvers (detumbling and satellite rotation) in a short time.

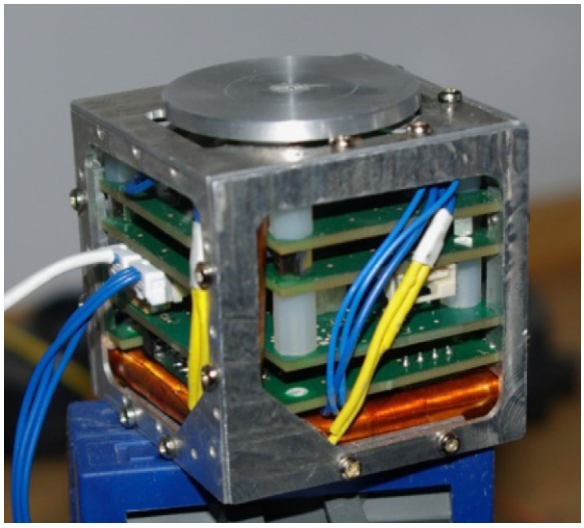

Fig. 15. Fully assembled prototype.

Fig. 15 shows the realized prototype: the three magnetorquers are visible on the front edge of the cube, while one of the three momentum wheels stays in the top face.

All electronics have been sized to fit on four boards inside the control system structure: magnetorquer controller, motor drivers, magnetometers and digital control. Power and serial communication use two connectors on one of the free sides of the cube.

Once the prototype has been assembled and fully programmed, a series of functional tests has been performed.

The first function tested has been the "*-Bdot*" control law to detumble the satellite. The system has been programmed to acquire a series of readings of the magnetic field each 0.5 s, perform a simple average filtering and calculate the current to be applied to the magnetorquers.

Results are shown in Fig. 16.

The graph contains the magnetometer readings on the *X*, *Y* and *Z* axes (bold long dashed, short dashed and solid lines, for *X*, *Y* and *Z* axes respectively), and the current imposed on magnetorquer read by internal sensors (thin dotted line, dashed and solid lines, for *X*, *Y* and *Z* axes respectively). It is clearly visible that the noise on the reading does not cause any false activation of the control, while during rotation the current is proportional to the derivate of the magnetic field variation, demonstrating the correctness of the filtering and applied parameters. The system was calibrated to read the magnetic field on the ground, but simply acting on the gain in the magnetometer circuits it is possible to calibrate it for space conditions.

Tests have also been performed on reaction wheels to determine the maximum available momentum. The motor without load has reached a speed of 15,000 rpm; with the load of the wheel the maximum available speed is 9000 rpm.

The acceleration and deceleration ramp is generated dynamically by the microcontroller, according to the

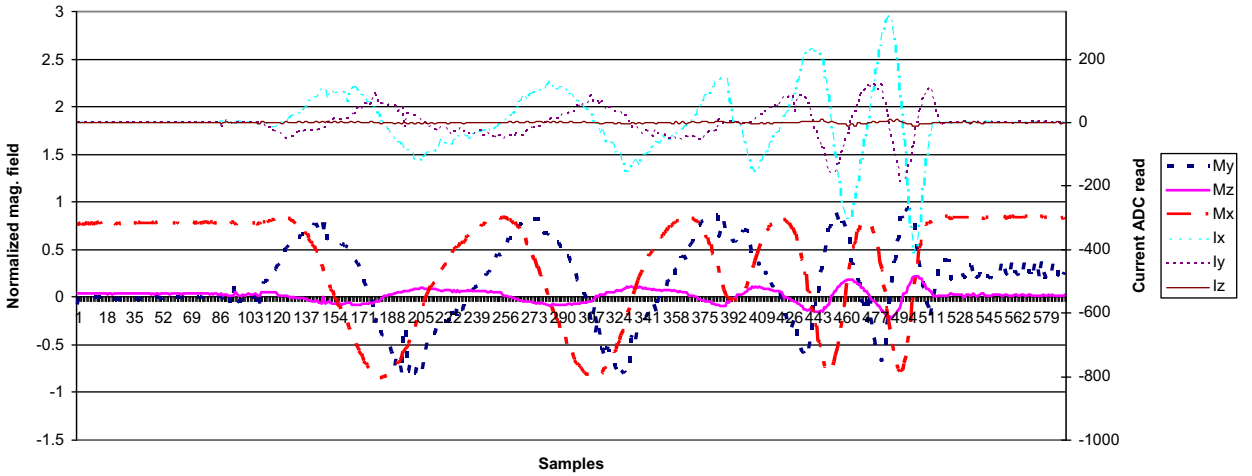

Fig. 16. Control law test for *X*, *Y* and *Z* axes.

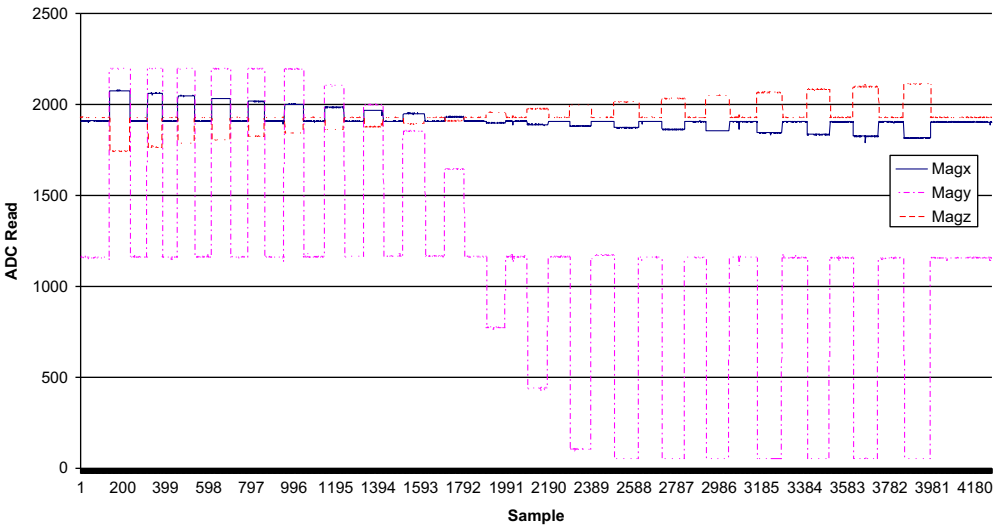

Fig. 17. Residual magnetization test.

speed of the motor, to use as best the internal clock generation hardware and minimize the torque required by each frequency step. Simulations have demonstrated the capability of the system to perform full rotation of the satellite in the conditions described before without saturation of the wheels.

A series of tests has been performed to evaluate the effect of residual magnetization in magnetorquer coils due to the extreme integration of different systems in a small volume. By comparing the magnetic field readings obtained between different current pulses applied to the magnetorquer, it has been possible to calculate the amplitude of the deviation due to the presence of the coil core.

Tests results are shown in Fig. 17, where the three components of the recorded magnetic fields are reported, with ADC counts on the *Y* axis and telemetry samples on the *X* axis. Each step corresponds to a current pulse through the coils, ranging from −100% to +100% at 10% steps.

Table 2
PSLV random vibration testing.

Frequency (Hz)	PSD (g^2/Hz)
20	0.002
110	0.002
250	0.034
1000	0.034
2000	0.009

By measuring the total excursion of the magnetometer and comparing these readings, it has been possible to create the following table:

The values reported in Tables 2 and 3 refer to the worst-case scenario, where two readings are performed

Table 3
Residual magnetization effects.

X axis max	*Y* axis max	*Z* axis max
1493	1626	1546
Residual Magnetization induced Offset for worst case		
3	18	2
% on axis maximum reading		
~0.3%	~1%	~0.2%

after two current pulses, one positive and one negative. As can be seen, the influence of the magnetorquer coils is negligible and well inside expected values, having an effect limited to 1% of the reading.

7. Conclusions

A 1U Cubesat system has been developed, aimed at student education, low cost realization and applied research. The system includes innovative solutions, potentially improving the overall performance, flexibility and cost. Ground test results show that these are all feasible and promising. These include: (i) structure made in ABS plastic by the rapid prototyping technique, (ii) photovoltaic system made of 3 J solar panels, assembled using an innovative gluing and electrical connection system, based on adhesive tin aluminum strips (iii) communication system based on commercial off-the-shelf transceivers and an antenna embedded in the plastic structure and (iv) miniaturized autonomous attitude control system ($5 \times 5 \times 5$ cm^3 volume).

References

[1] J. Piattoni, G.P. Candini, G. Pezzi, F. Santoni, F. Piergentili, Plastic cubesat: an innovative and low-cost way to perform research and hands-on education, IAC-11, E1,5,8 62nd International Astronautical Congress, October 2011, Cape Town, South Africa.
[2] K.T. Ulrich, S.D. Eppinger, Product Design and Development, third edition, McGraw-Hill, 2004.
[3] W. Guangchun, L. Huiping, G. Yanjin, Z. Guoqun, A rapid design and manufacturing system for product development applications, Rapid Prototyping J. 10 (3) (2004) 200–206.
[4] M.A. Evans, R.I. Campbell, A comparative evaluation of industrial design models produced using rapid prototyping and workshop-based fabrication techniques, Rapid Prototyping J. 9 (5) (2003) 344–351.
[5] N. Hopkinson, P.M. Dickens, Rapid prototyping for direct manufacture, Rapid Prototyping J. 7 (4) (2001) 197–202.
[6] S. Tennyson, G. McCain, S. Hatten, R. Eggert, Case study: promoting design automation by rural manufacturers, Rapid Prototyping J. 12 (5) (2006) 304–309.
[7] P. Rochus, J.-Y. Plesseria, M. Van Elsen, J.-P. Kruth, R. Carrusc, T. Dormalc, New applications of rapid prototyping and rapid manufacturing (RP/RM) technologies for space instrumentation, Acta Astronaut. 61 (1–6) (2007) 352–359, http://dx.doi.org/10.1016/j.actaastro. 2007.01.004.
[8] Anna Bellini, Selçuk Güçeri, Mechanical characterization of parts fabricated using fused deposition modeling, Rapid Prototyping J. 9 (4) (2003) 252–264.
[9] Jordi Puig-Suari, Clark Turner, Robert J. Twiggs, CubeSat: the development and launch support infrastructure for eighteen different satellite customers on one launch, in: Proceedings of the 15th Annual/USU Conference on Small Satellites, August 2002, Logan, UT.
[10] M.L. Battagliere, G.P. Candini, J. Piattoni, E. Paolini, F. Santoni, F. Piergentili, The BUGS experiment: overview and in-flight results, in: Proceedings of the REXUS/BEXUS Experimental Results Symposium, 23–24 June, Bremen, Germany.
[11] M.L. Battagliere, G.P. Candini, J. Piattoni, E. Paolini, F. Piergentili, Post-flight data analysis of the bugs experiment on sounding rocket REXUS-7, IAC 10-A2.3.7, 61th International Astronautical Congress, 27 September–1 October 2010, Prague, Czech Republic.
[12] F. Santoni, F. Piergentili, Analysis of the UNISAT-3 solar array in-orbit performance, J. Spacecr. Rockets 45 142–148, AIAA, ISSN: 0022-4650.
[13] F. Santoni, F. Piergentili, F. Graziani, The UNISAT program: lessons learned and achieved results, Acta Astronaut. 65 (2009) 54–60. (ELSEVIER, ISSN: 0094-5765).
[14] NASA Space Vehicle Design Criteria (Structure), NASA SP-8053, June 1970.
[15] W.J. Larson, J.R. Wertz, Space Mission Analysis and Design, third edition, Space Technology Library-Microcosm Press, California, 2004.